Boletim da Sociedade Astronômica Brasileira, **35**, no. 1, 278-282

The co-evolution of central galaxies and AGN activity in different environments

V. M. Sampaio,[1,2] A. Aragón-Salamanca,[2] M. R. Merrifield,[2], R. R. de Carvalho ,[1] I. Ferreras,[3,4,5], S. Zhou[2]

[1] NAT - Universidade Cruzeiro do Sul / Universidade Cidade de São Paulo, 01506-000, SP, Brazil e-mail: vitorms999@gmail.com
[2] School of Physics and Astronomy, University of Nottingham, University Park, Nottingham NG7 2RD, UK
[3] Instituto de Astrofísica de Canarias, Calle Vía Láctea s/n, E38205, La Laguna, Tenerife, Spain
[4] Department of Physics and Astronomy, University College London, Gower Street, London WC1E 6BT, UK
[5] Departamento de Astrofísica, Universidad de La Laguna, E38206 La Laguna, Tenerife, Spain

Abstract. We study 80,000 SDSS central galaxies to explore AGN feedback effects on their evolution. Optically-selected AGN (Seyferts) prevalence rises with stellar mass, surpassing star-formation for $M_{stellar} \geq 10^{11} M_{\odot}$ galaxies. AGN fraction varies with star-formation activity, peaking near the green valley ($\sim 17 \pm 4\%$) within the blue cloud and decreasing in the red sequence. This trend supports AGN feedback's role in regulating star formation. Exploring morphology, we show that Seyfert centrals have early-type morphology with residual star formation, transitioning from late- to early-type before complete quenching. Stellar mass influences this transformation; low-mass systems shift to elliptical morphology even before the green valley, whereas high-mass ones maintain spirals until the beginning of the red sequence. In high-stellar-mass centrals, Seyfert fraction rises from early- to late-type, suggesting a link between AGN feedback and morphology. Our analysis indicates that AGN are fueled by host halo gas, and, when in group centrals, by interactions with satellite galaxies.

Resumo. Estudamos 80.000 galáxias centrais do SDSS para entender o impacto do feedback do AGN em sua evolução. A prevalência de AGN opticamente selecionados (Seyferts) aumenta com a massa estelar, ultrapassando a formação estelar para galáxias com $M_{stellar} \geq 10^{11} M_{\odot}$. A fração de AGN varia com a atividade de formação estelar, atingindo o pico próximo ao *Green Valley* ($\sim 17 \pm 4\%$) e diminuindo na *Red Sequence*. Essa tendência apoia o papel do feedback do AGN na regulação da formação estelar. Ao explorar morfologia, mostramos que as galáxias centrais Seyfert têm uma morfologia do tipo *early-type* com formação estelar residual, fazendo a transição de *late-* para *early-type* antes da extinção completa da formação estelar. A massa estelar influencia essa transformação; sistemas de baixa massa mudam para uma morfologia elíptica mesmo antes do *Green Valley*, enquanto os de alta massa mantêm padrões espirais até o início da *Red Sequence*. Nas galáxias centrais de alta massa estelar, há um excesso na fração de Seyferts em espirais, sugerindo uma ligação entre o feedback do AGN e a morfologia. Nossa análise indica que os AGN são alimentados pelo gás do halo hospedeiro da galáxia e, quando em galáxias centrais massivas de grupos, por interações com galáxias satélites.

Keywords. Galaxies: clusters: general – Galaxies: evolution – Galaxies: general

1. Introduction

In recent decades, astronomers have concentrated on unraveling the diverse mechanisms steering galaxy evolution throughout cosmic time. The persistent bimodality observed in various galaxy properties, such as colors and star-formation rates , serves as both a crucial piece of evidence and a significant challenge for any theory aiming to explain galaxy formation and evolution (e.g. Wetzel, Tinker, & Conroy 2012).

Galaxies fall into distinct categories: the blue cloud (BC), characterized by blue, star-forming galaxies with late-type morphologies (late-type galaxies, LTGs); the red sequence (RS), comprising red galaxies with minimal or no star formation, primarily featuring early-type morphologies (early-type galaxies, ETGs); and the green valley (GV), an intermediate class with galaxies exhibiting intermediate colors, reduced star formation, and a variety of morphologies. Despite numerous attempts (e.g. Trussler et al 2020) to elucidate the transition from the BC through the GV ans subsequently to the RS by invoking various physical mechanisms to suppress star formation and alter morphology, a definitive answer is yet to be discovered.

A fundamental factor influencing galaxy evolution is the presence of a central super-massive black hole (SMBH). According to Dubois et al. (2013), SMBH mass stands out as a highly effective predictor of whether a galaxy is actively forming stars or in a quenched state. Some theories, such as CRIS, propose that the correlation between SMBH mass and star formation suppression is attributed to the impact of an active galactic nucleus (AGN) on the galaxy's interstellar medium, commonly referred to as 'AGN feedback.' The influence of an AGN is contingent on both the SMBH's mass at its core and the quantity and rate of 'fuel' it receives.

Empirically, Magorrian et al (1998) demonstrated a positive correlation between SMBH mass and the central stellar velocity dispersion of the host galaxy ($\sigma_{\rm galaxy}$). Additionally, other studies find an increasing fraction of quenched galaxies with a rise in $\sigma_{\rm galaxy}$ (e.g. Bluck et al. 2016). Given that cluster centrals typically exhibit the highest $\sigma_{\rm galaxy}$, it is anticipated that they harbor the most massive SMBHs, suggesting pronounced suppression of star formation.

With the extensive dataset from the Sloan Digital Sky Survey (SDSS), we explore the demographics of optically-identified AGN (via BPT diagram) in both isolated and group/cluster central galaxies. Our focus is on understanding the interplay between internal and environmental factors influencing AGN and their fueling mechanisms. Initially, we categorize galaxies based on their environment and employ the BPT diagram to examine the fraction of strong AGN (Seyfert galaxies) in different settings. We consider additional factors such as galaxy mass, morphology, central velocity dispersion, and host halo mass. These

factors, along with environmental information, are linked to the AGN and star-formation activity of galaxies. Our objective is to identify the physical processes fueling AGN, driving star-formation activity, and causing both star-formation quenching and morphological transitions.

2. Data selection and methods

We utilize single-fibre spectroscopy data from the Sloan Digital Sky Survey Sixteenth Data Release (SDSS-DR16 Abazajian et al. 2009). Our sample is confined to the redshift range $0.03 \leq z \leq 0.1$. The lower limit is set to mitigate aperture biases in measured galaxy properties arising from the fixed 3 arc-sec fiber diameter. To ensure completeness, we only include galaxies with apparent Petrosian magnitude in the r-band brighter than 17.78, corresponding to the survey's spectroscopic completeness limit at $z = 0.1$. Additionally, a signal-to-noise ratio (S/N)[1] threshold of 10 is imposed to guarantee adequate spectral quality.

2.1. Environmental classification

From these data, we select central galaxies using the Yang catalogue (Yang et al. 2007). This catalogue was built by applying a halo finder algorithm (Yang et al. 2005) to the New York University Value Added Galaxy Catalogue (Blanton et al. 2005). Galaxies in the same halo are considered to be part of the same group/cluster. This allows us to define different environments for central galaxies:

1. Isolated centrals – galaxies living in halos occupied by a single galaxy ($N_{members} = 1$);
2. Binary system centrals – the most massive galaxy of a pair hosted in the same halo ($N_{members} = 2$);
3. Group centrals – central galaxies in halos occupied by at least 3 galaxies, but no more than 10 ($3 \leq N_{members} < 10$);
4. Cluster centrals – the central system in halos populated by more than 10 member galaxies ($N_{members} > 10$).

For halos hosting more than one galaxy, we define the central system to be the most massive one, with stellar mass calculated via equation (2) in Yang et al. (2005). We tested how the sample would change if we selected the brightest cluster galaxy (BCG) instead; we find no significant differences, since 98.2% of the most massive galaxies are also BCGs. We further guarantee completeness regarding the halo mass estimate by imposing the conservative threshold presented in Yang et al. (2007),

$$\log(M_{halo}/M_{\odot}) \geq 12 + \frac{z_c - 0.085}{0.069}, \quad (1)$$

where z_c denotes the median redshift of a given system (halo), and M_{halo} is the halos mass estimate.

2.2. Spectra derived quantities and BPT diagram

The galaxies' stellar mass ($M_{stellar}$), star formation rate (SFR), and velocity dispersion ($\sigma_g$alaxy) are retrieved from the Max Planck Institut fur Astrophysik – John Hopkins University catalogue (MPA-JHU Brinchmann et al. 2004). This catalogue offers reliable measurements and associated errors for galaxies in SDSS–DR8 without spectral anomalies. Notably, it employs a unique method to estimate the galaxies' SFR. Initially, the SFR is derived using the Hα emission-line flux for galaxies classified as 'star-forming' in the BPT diagram. Subsequently, this estimation is extrapolated to other galaxies using a calibration between SFR and the 4000Å break. This approach is crucial in our study as it ensures that SFR estimates are not contaminated by potential AGN contributions to the Hα flux. In Fig. 1 we show the distribution of halo mass as a function of redshift, for the four subsamples aforementioned. We also colour the points according to stellar mass and show as a black dashed line the limit imposed by Eq. 1.

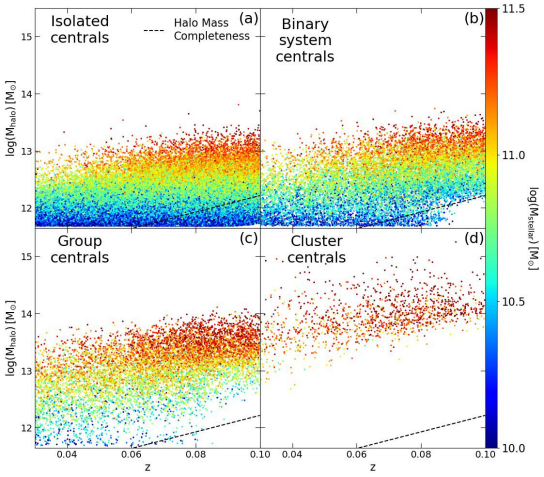

Figure 1. Distribution of halo mass as a function of redshift. We separate galaxies in the four subsamples aforementioned. Data is coloured according to stellar mass. The black dashed line show the limit imposed by Eq. 1.

Furthermore, the MPA–JHU catalogue classifies galaxies using the BPT diagram (Baldwin et al. 1981), resulting in six categories: 1) star-forming, 2) low S/N star-forming, 3) composite, 4) Seyfert, 5) LINER, and 6) unclassified. The 'unclassified' category includes galaxies with unreliable BPT classification due to at least one emission line having S/N < 3. To ensure robust results, we only consider galaxies with Hα equivalent width (EW(Hα) >3Å), following the WHAN diagram Cid Fernandes et al. (2010) threshold. This avoids contamination from galaxies with weak emission lines, preventing influence from underlying stellar absorption lines. The combined sample of 'unclassified' galaxies and those with EW(Hα) $\leq$ 3Å is denoted as 'Passive+Retired' (P+R) galaxies, characterized by negligible star formation. We hereon use this combined BPT+WHAN definition to select Seyfert galaxies. We also discard LINERS, as their ionization is well explained by the presence of hot old stars.

2.3. Morphological characterization

Also of relevance, when galaxies undergo changes in their star-formation properties, their morphologies can also evolve. In this study, we utilize the T-Type parameter, initially introduced by (de Vaucouleurs 1963), to classify lenticular systems. For our analysis, we find it convenient to use a modified T-Type parameter that exhibits continuous variation from −3 to 6, as opposed to the original discrete values. Typically, a T-Type value ≤ 0 indicates an early-type galaxy, while T-Type values > 0 correspond to late-type morphologies. We therefore adopt the T-Type values from Domínguez Sánchez et al. (2018), derived using a deep-learning convolutional neural network algorithm applied to 670,722 galaxies from the SDSS-DR7 database.

[1] Median signal-to-noise ratio of all good pixels in the galaxy spectrum.

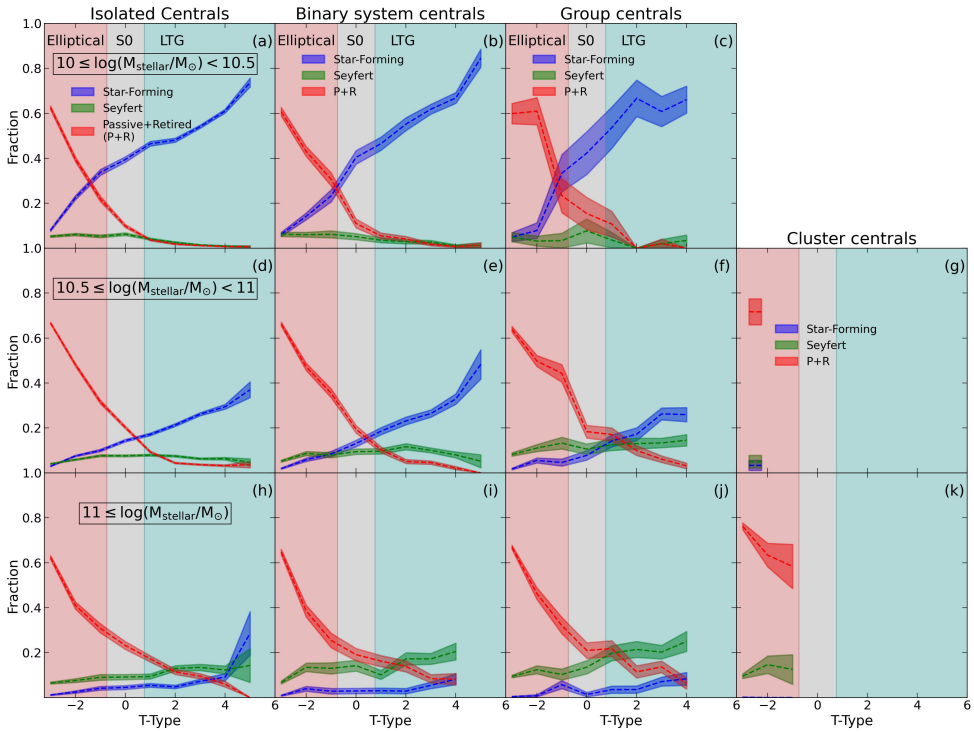

Figure 2. The fraction of star forming (blue), Seyfert (green) and passive+retired (P+R, red) galaxies as a function of morphology (T-Type). We separate galaxies according to their environmental richness and into 4 different stellar mass bins. Background color represent the related morphology (spiral, S0, elliptical), as can be seen in panel (a).

3. Demographics: Where Seyferts live?

3.1. The role of Morphology

In Fig. 2, we present the Seyfert fraction as a function of the T-Type of host galaxies, alongside the fractions of star-forming and P+R galaxies for context. To ensure reliability, a minimum of 20 galaxies per bin is imposed for calculating the relevant fractions. Three T-Type ranges are defined for reference: $-3 \leq T\!-\!Type < -0.75$ corresponds to elliptical galaxies; $-0.75 \leq T\!-\!Type \leq 0.75$ to lenticular (S0) galaxies; and $0.75 < T\!-\!Type \leq 6$ to spiral galaxies. These limits accommodate uncertainties in T-Type (ΔT-Type, $\sim$ 0.5), with changes in bin boundaries of this size not significantly impacting results.

High stellar masses show a significantly higher Seyfert fraction than low-mass galaxies, averaging 5±3% in the lower stellar mass bin and 13 ± 4% in the higher bin across all environments. In the most massive bin, Seyferts outnumber star-forming galaxies in all morphologies and environments, with over twice as many high-mass galaxies classified as Seyferts, even among late-type spirals. This suggests that, in the absence of star formation as an ionizing mechanism, even modest AGN activity becomes apparent, potentially indicating a link between AGN activity and the suppression of star formation in massive galaxies. Finally, the declining Seyfert fraction during the transition from spirals to ETGs lends support to the notion that AGN feedback influences the morphological transition process and contributes to the observed morphological diversity in present-day galaxies.

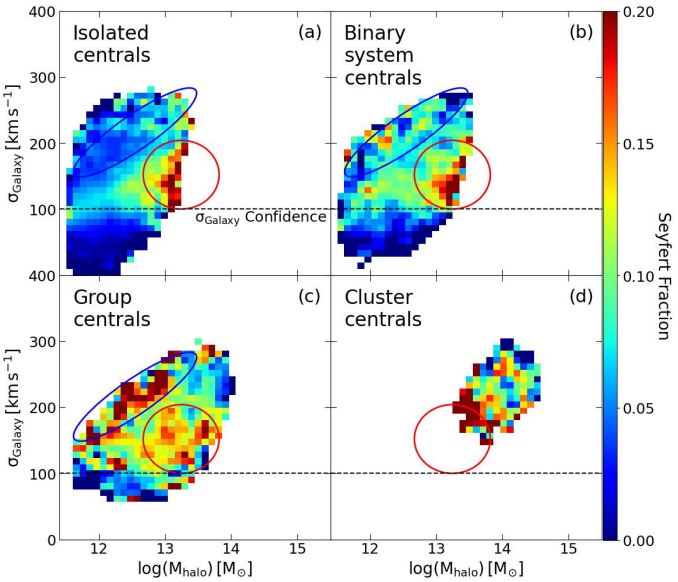

Figure 3. The distribution of the Seyfert fraction in the M_{halo} vs. σ_{galaxy}. We divide galaxies only regarding environmental richness, as stellar mass bins would be the same as slicing the diagram vertically. The blue and red ellipses highlight high Seyfert fraction regions.

3.2. The Fueling of AGN

AGN fueling may depend on a combination of both internal and environmental properties. In Fig. 3, we depict the median Seyfert fraction in the σ_{galaxy} vs. M_{halo} plane for central galaxies across different environments. Using a bootstrap technique, we calculate the median Seyfert fraction and its uncertainty for each pixel. Our analysis focuses on galaxies with $\sigma_{galaxy} > 100$,km/s, as values below this threshold in the MPA-JHU catalogue become unreliable due to SDSS spectra resolution. To confirm the trend's robustness, we repeated the analysis with 50% larger bins, yielding consistent results. Still, we present raw binned

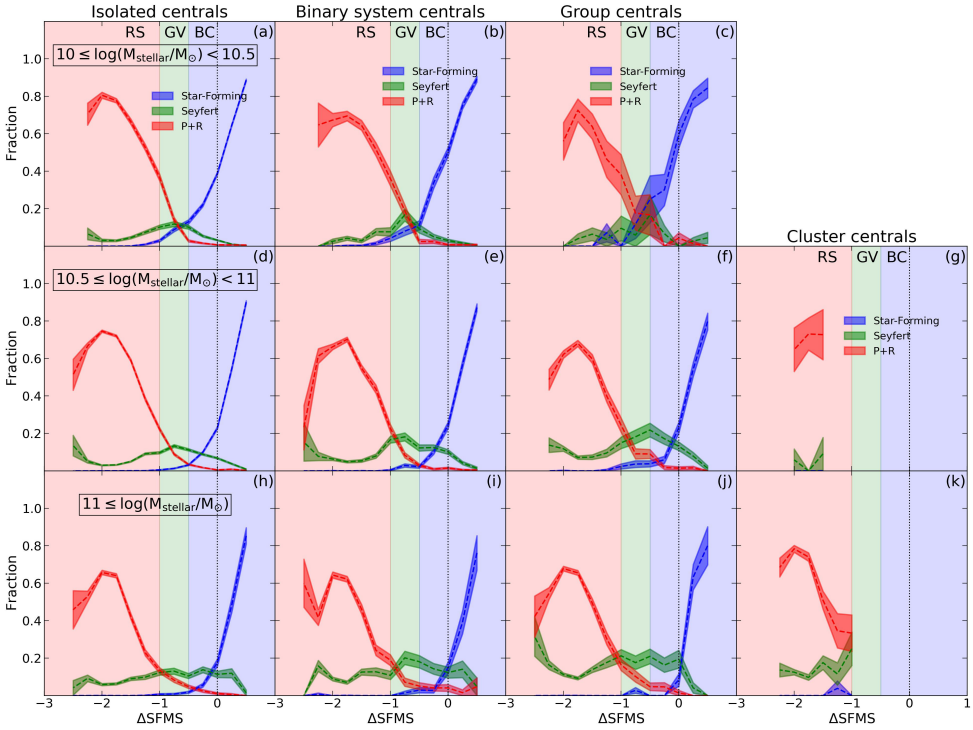

Figure 4. The fraction of star forming (blue), Seyfert (green) and P+R galaxies as a function of the vertical distance to the star formation main sequence (ΔSFMS). We separate central galaxies according to environmental richness and stellar mass. The background colors represent the BC, GV and RS regions.

density maps without smoothing for a more accurate representation of data and uncertainties.

n Fig. 3 (a), the highest Seyfert fraction among isolated centrals is observed in galaxies residing in the most massive halos ($M_{halo} \geq 10^{13} M_{\odot}$) with intermediate velocity dispersions ($100 \leq \sigma_{galaxy} \leq 200$,km,s^{-1}). This pattern, marked by red circles, is similarly observed in the other panels. Suggesting fueling through the accreted gas from its own host halo. Complementary, in Fig. 3 (c), group centrals exhibit a second region with a notable Seyfert fraction (marked by the blue ellipse). These are galaxies with relatively high velocity dispersion for their halo masses. Within this region, Seyfert fraction systematically decreases from group centrals to binary system and isolated ones. In this region, the environment influences AGN fuelling, and for group centrals, Seyferts are predominantly found in galaxies with high σ_{galaxy}, suggesting that a larger SMBH mass increases the likelihood of AGN activity, even with the same gas reservoir. These high velocity dispersion galaxies tend to be ETGs. The prevalence of this phenomenon in the group environment may indicate that group centrals are more prone to recent interactions with other galaxies, particularly their satellites, compared to isolated centrals and those in binary systems.

4. The impact of AGN activity in central galaxies

To detail the role of AGN activity in driving galaxies from the BC to the RS, we investigate the fraction of Seyferts and their respective morphology as a function of the vertical distance from the star formation main sequence (ΔSFMS). By adopting this approach, we make our analysis weakly dependent on the definition of BC, GV and RS boundaries. Fig.4 shows galaxy type fraction variation based on vertical distance to the SFMS for diverse environments and stellar-mass ranges, with analysis limited to bins containing at least 20 galaxies.

4.1. AGN as driver of Star Formation Quenching

Results in Fig. 4 offer a fresh perspective on AGN activity's potential impact on central galaxy evolution. The rising Seyfert fraction across the BC, moving away from the SFMS, aligns with a concurrent decrease in the star-forming fraction. This suggests that, despite comprising only 10-20 of central galaxies, AGN feedback could be highly effective at quenching star formation across all stellar masses. In this scenario, the AGN triggers a reduction in star formation, with a time delay before its radiation becomes the primary ISM ionization source. The AGN activity becomes apparent after the associated star formation decrease diminishes the ionizing effect of high-mass stars.

Furthermore, we notice a noteworthy trend in the RS. ETGs are commonly associated with the red sequence and considered to be passively evolving, often referred to as "red and dead," indicating halted star formation and aging stellar populations. However, by examining the Seyfert fraction based on ΔSFMS, our findings challenge the notion that all central galaxies in the red sequence are entirely inactive. In Fig. 4, specifically in panel (h), we observe that a significant fraction (approximately one-third) of the most massive group galaxies with the lowest star-formation activity host AGN. This substantial AGN presence aligns with our prior results, suggesting that massive central galaxies in groups (typically ellipticals) can receive gas through interactions with satellite galaxies, leading to AGN activity.

4.2. The Impact of AGN activity in Galaxy Morphology

Tracking Seyfert galaxies' morphology in relation to their star-formation activity allows us to investigate whether AGN feedback influences their host galaxies' star formation before or after a morphological change. Fig. 5 displays the median T-Type of Seyfert galaxies concerning ΔSFMS, categorized by stellar mass and environmental richness. For group and cluster centrals, only

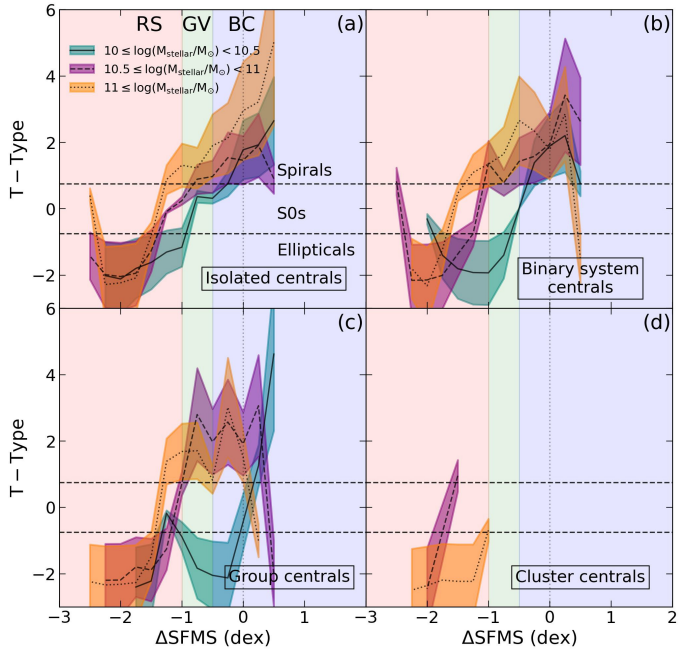

Figure 5. Similar to Fig. 4, but for the variation in T-Type, and only focusing in Seyferts.

curves with a minimum of 10 galaxies per bin are shown to mitigate statistical uncertainties.

Statistically, Seyfert galaxies tend to attain elliptical morphologies (median T-Type ~ -2) before their star-formation is fully suppressed (i.e., before reaching the core of the RS region, ΔSFMS ~ -2). There is a mass-dependent trend in the morphological transition of Seyfert galaxies: low-mass galaxies typically transition from the GV with elliptical morphologies (regardless of environmental richness), intermediate-mass systems tend to emerge as S0s, and high-mass systems often maintain spiral morphologies beyond the GV. This implies that AGN activity can be more influential in the morphological transition of low-mass galaxies, while more massive systems retain their morphology for an extended ΔSFMS.

5. Conclusions

- AGN-driven ionisation surpasses star-formation ionisation in $M_{stellar} \geq 10^{11} M_\odot$ galaxies, irrespective of environment. At these high masses, LTGs with Seyfert activity reach $21 \pm 4\%$ in group centrals, while only $7 \pm 3\%$ have their interstellar medium ionized by star formation.
- In high stellar mass central galaxies, Seyfert fraction increases with T-Type, from 5 ± 1 at T-Type~ -2.5 to 18 ± 3 at T-Type~ 4. This suggests a link between AGN feedback and morphology. Low-mass galaxies, regardless of morphology and environment, have a low Seyfert fraction due to their inability to fuel star-formation and AGN simultaneously.
- Seyfert fraction variation with velocity dispersion and halo mass implies two AGN fueling mechanisms: reliance on host halo gas reservoir (more efficient with increasing halo mass) and gas reservoir increase via interactions with satellite systems. The latter is crucial for the evolution of high-mass centrals in groups and low-mass clusters.
- Seyfert fraction changes systematically with star-formation activity. Within the blue cloud, it increases as star-formation declines, reaching a peak in the green valley. High mass group centrals show a peak Seyfert fraction of $18 \pm 4\%$ near the green valley, decreasing as galaxies transition to the red sequence. This suggests AGN feedback regulates and suppresses star-formation.
- Tracing Seyfert central galaxies' morphology with star-formation activity, they typically have an early-type morphology while hosting residual star formation. In all environments, Seyfert galaxies evolve from late- to early-type before complete star formation quenching. Stellar mass is crucial; low mass systems tend towards elliptical morphology even before the green valley, while high-mass ones maintain a spiral morphology until the beginning of the red sequence.

Acknowledgements. VMS and RRdC acknowledge the support from FAPESP through the grants 2020/16243-3, 2020/15245-2 and 2021/13683-5. SZ, MRM, and AAS acknowledge financial support from the UK Science and Technology Facilities Council (STFC; grant ref: ST/T000171/1). IF acknowledges support from the Spanish Ministry of Science, Innovation and Universities (MCIU), through grant PID2019-104788GB-I00.

References

Abazajian, K. N., et al. 2009, ApJS, 182, 543
Baldwin, J. A., Phillips, M. M., & Terlevich, R. 1981, PASP, 93, 5
Blanton, M. R., et al. 2005, AJ, 129, 2562
Bluck, A. F., et al. 2016, MNRAS, 462, 2559
Brinchmann, J., et al. 2004, MNRAS, 351, 1151
Fernandes, R. C., et al. 2010, MNRAS, 403, 1036
Domínguez Sánchez, H., et a. 2018, MNRAS, 476, 3661
Dubois, Y., et al. 2013, MNRAS, 433, 3297
Magorrian, J., et al. 1998, AJ, 115, 2285
Trussler, J., et al. 2020, MNRAS, 491, 5406
De Vaucouleurs, G. 1963, ApJS, 8, 31
Yang, X., et al. 2005, MNRAS, 356, 1293
Yang, X., et al. 2007, ApJ, 671, 153
Wetzel, A. R., Tinker, J. L., & Conroy, C. 2012, MNRAS, 424, 232